NJC

LETTER

View Article Online
View Journal | View Issue

Cite this: *New J. Chem.*, 2016, **40**, 9012

Received (in Victoria, Australia) 10th May 2016,
Accepted 12th September 2016

DOI: 10.1039/c6nj01472k

www.rsc.org/njc

High temperature spin crossover in [Fe(pyrazine){Ag(CN)$_2$}$_2$] and its solvate†

Il'ya A. Gural'skiy,*[ab] Sergii I. Shylin,[ab] Bohdan O. Golub,[a] Vadim Ksenofontov,[b] Igor O. Fritsky[a] and Wolfgang Tremel[b]

A high temperature spin crossover (T_{up} = 367 K) was detected in a metal–organic framework [Fe(pz){Ag(CN)$_2$}$_2$]·MeCN (pz = pyrazine). Upon heating, this solvate released acetonitrile guest molecules, which slightly shifted the transition temperature of the complex (T_{up} = 370 K and T_{down} = 356 K).

The existence of two possible spin states in the family of 3d^4–3d^7 metal complexes provokes a spectacular spin transition phenomenon – an ability to display molecular bistability driven by diverse external stimuli.[1] Current investigations of spin crossover (SCO) are mostly focused on the development of novel SCO coordination compounds, theoretical understanding of the phenomenon, elaboration and procession of SCO nano- and composite materials, and implementation of these materials for photonic, electronic and mechanical devices, and sensors.[2,3] Iron(II) SCO attracts considerable attention due to the wide variety of SCO complexes it forms; consequently, a range of temperatures, abruptness, hysteresis and completeness of the spin transition are available according to the desired application. SCO in iron(II) occurs between the diamagnetic (S = 0) low-spin (LS) state (with all d-electrons coupled – $t_{2g}^6e_g^0$) and paramagnetic (S = 2) high-spin (HS) state (with four d-electrons unpaired – $t_{2g}^4e_g^2$). Crossover below room temperature is more common for entropy-driven thermal transitions, whereas transitions at elevated temperatures are found just in a few selected families[4–6] or distinct examples.[7–14]

Among all iron(II) SCO complexes, Hofmann-clathrate-like frameworks attract attention due to their simplicity, universal design approach, spectacular guest effect that can drastically change their SCO behaviour, and the possibility of elevated transition temperatures.[5] The key elements of their structures are cyanoheterometallic layers supported by N-donor organic heterocyclic ligands. The first metal is iron, whereas the second can be Ni(II), Pd(II), Pt(II), Cu(I), Ag(I), Au(I), Cr(III) or Nb(IV). Both the structure of the ligand and the nature of the second metal define the final geometry of the network. Thus, the first clathrate-like SCO framework was a 2D coordination polymer, Fe(pyridine)$_2$Ni(CN)$_4$, obtained by Kitazawa *et al.*[15] The highly symmetric 3D frameworks [Fe(L)Ni(CN)$_4$], which featured square-planar coordinated Ni, Pd and Pt, and bidentate ligands, along with pores accessible to guest molecules, were obtained by Real *et al.*[16] Thus, the inclusion of certain inorganic and organic molecules into Hofmann-clathrate-like frameworks, such as CS_2,[17] benzene, SO_2,[18] alcohols, acetone, acetonitrile, toluene,[19] thiourea,[20] phenazine, anthracene, naphtaline,[21] thiophene, furan, and pyrol,[22] can considerably tune the SCO behaviour of the complexes. More complicated 3D architectures can be constructed starting from tripodal ligands.[23]

Even though there are many recent examples of SCO complexes of diverse architectures, we believe special attention should be paid to simple and easily accessible compounds that, at the same time, may exhibit very original SCO behaviour. Pyrazine[7,16] and its derivatives[24] have been used as ligands for constructing SCO MOFs. In this letter, we describe a temperature induced SCO in the complex [Fe(pz){Ag(CN)$_2$}$_2$], whose structure and magnetic behaviour below 300 K were reported in 2002 by Real *et al.*,[25] and its solvate with acetonitrile. Both species possess a molecular bistability at elevated temperatures.

The complex [Fe(pz){Ag(CN)$_2$}$_2$]·MeCN (**1·MeCN**) was obtained starting from iron(II) perchlorate, potassium dicyanoargentate and pyrazine in a water–acetonitrile mixture. The general structure of the framework is similar to the one reported by Real *et al.*;[25] however, the pores within our complex are filled with acetonitrile molecules. A comparison of the two networks is given in Fig. S1 (ESI†). The coordination environment of the iron(II) centres, as is typical for SCO analogues of Hofmann clathrates, comprises four cyanometallates and two pyrazine

[a] *Department of Chemistry, Taras Shevchenko National University of Kyiv, Volodymyrska St. 64/13, Kyiv 01601, Ukraine. E-mail: illia.guralskyi@univ.kiev.ua*
[b] *Institute of Inorganic and Analytical Chemistry, Johannes Gutenberg University of Mainz, Staudingerweg 9, Mainz 55099, Germany*

† Electronic supplementary information (ESI) available: Experimental details, crystallographic tables, powder diffractograms. CCDC 1478973. For ESI and crystallographic data in CIF or other electronic format see DOI: 10.1039/c6nj01472k

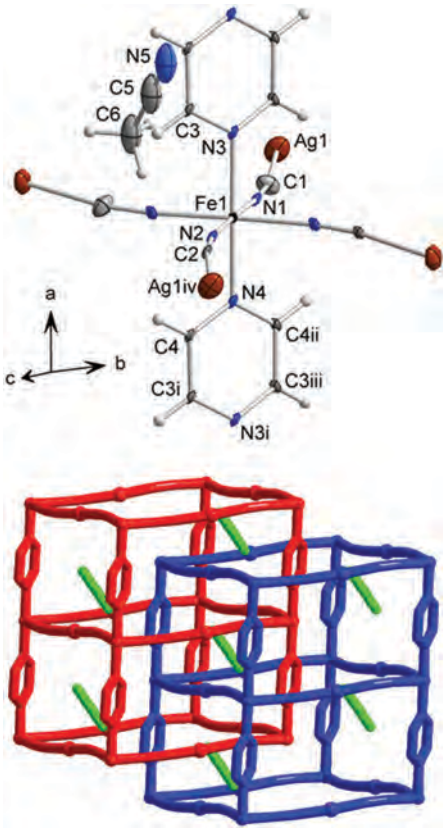

Fig. 1 (top) ORTEP view of the crystal structure of **1·MeCN** (C – gray, N – blue, Fe – black, and Ag – orange). i: $-1+x; y; z$. ii: $x; -1-y; z$. iii: $-1+x; -1-y; z$. iv: $-0.5+x; -0.5+y; -1+z$. (bottom) Hofmann-clathrate-like structure is built of cyanoheterometallic layers connected by bridging μ_2-pyrazine. Two identical networks are interpenetrated and the residual space is filled in with acetonitrile molecules.

ligands. This invokes a spin transition behaviour in both **1** and **1·MeCN**.

1·MeCN crystallizes in the space group *Cm* (Fig. 1). The iron atoms are located on a special position and the corresponding metal–cyanide layers propagate in the *bc* plane. They are connected by *N*,*N*′-bridging pyrazine ligands that link iron sites along the *a*-axis. Two identical frameworks interpenetrate to form a rigid structure that has small pores available for acetonitrile molecules. An analogous gold(I) complex[7] exists with a very similar structure, consisting of a network with pyrazine ligands disordered between two positions; this protects its framework from any solvent inclusion.

The iron to ligand distances (Fe–N_{CN} = 1.92(2) and 1.94(2) Å, Fe–N_{pz} = 1.98(2) and 2.00(2) Å) are indicative of the LS state of the metallic centres. A polyhedral distortion consisting of a deviation from octahedral geometry, $\sum|90^\circ - \Theta_{N-Fe-N}|$ = 9.0(81)°, is within the typical range for LS Fe(II). Acetonitrile molecules do not show any considerable interactions, even where there are N_{MeCN}–π_{pz} contacts (N5–centroid#1 = 3.05(4) Å, N5–centroid#1–N3 = 87(2)°) and N_{MeCN}–Ag contacts (N5–Ag1 = 3.13(2) Å). Possible CH–π_{pz} contacts should also be taken into account (C6–centroid#2 = 3.30(5) Å). Detailed crystallographic data are provided in the ESI.† Powder diffractometry (Fig. S2, ESI†)

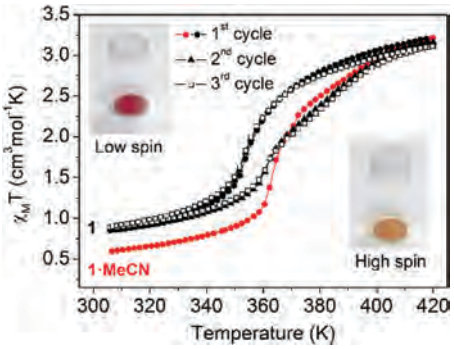

Fig. 2 Temperature dependent magnetic measurements of the complex in three consecutive thermal cycles. Heating branch of the first cycle corresponds to the transition in **1·MeCN**, whereas the loss of acetonitrile causes a shift of SCO temperature in **1** and an increase of the HS state fraction at low temperatures. Photographs of **1** in both spin states are inserted.

reveals no considerable structural changes after the framework loses its acetonitrile molecules when heated for 15 min at 393 K.

Temperature dependent magnetic measurements of the complex within the 306–420 K region are given in Fig. 2 and Fig. S3 (ESI†).

At 306 K, **1·MeCN** is in its LS state with χT_{306K} = 0.59 cm^3 mol^{-1} K. A gradual evolution of magnetic susceptibility upon heating signals a spin transition, with a major crossover taking place above 350 K and $T_{1/2}^{up}$ = 367 K. At 420 K, the framework is in its HS form with χT_{420K} = 3.23 cm^3 mol^{-1} K. The thermal treatment is also accompanied by a loss of acetonitrile guest molecules. The subsequent two cycles show only a small difference compared to the transition of the solvated framework.

The LS to HS transition of **1** has a more gradual nature, even though the transition temperature is almost unchanged ($T_{1/2}^{up}$ = 370 K). The reverse HS to LS transition occurs at $T_{1/2}^{down} \sim$ 356 K and corresponds to a hysteresis loop of 14 K. The χT_{306K} of 0.86 cm^3 mol^{-1} K for **1** is slightly higher than that of **1·MeCN**. This is due to the residual HS (non SCO) fraction that emerges at room temperature after thermal treatment (see below). As a result, thermal cycles corresponding to the behaviour of this framework without solvent (**1**) are reproducible.

Compared to the gold(I) analogue – [Fe(pz){Au(CN)$_2$}$_2$] – the SCO in **1** also occurs well above room temperature, but the transition is less abrupt. The evolution of the SCO curve in the first heating cycle, which is not observed in the Au(I) complex,[7] is caused by the presence of the guest solvent molecules.

Thermogravimetric measurements (TGA, Fig. 3) indicate a stepwise decomposition of the framework between 273 and 873 K. The initial mass loss occurs in two steps with an overall weight loss exceeding one solvent molecule per one iron centre (10.4% exp. *vs.* 8.2% theor.). This is probably due to the surface/inter-grain solvent content. Subsequent heating triggers pyrazine loss that continues up to 540 K (16.1% exp. *vs.* 16.1% theor.). The final two-step weight loss corresponds to the release of cyanide (17.5% exp. *vs.* 20.9% theor.). The residue corresponds to the Fe–Ag content (*ca.* 55% exp. *vs.* 54.7% theor.). Small endothermic peaks at 300–400 K originate from solvent loss and the SCO, whereas the pyrazine loss causes an

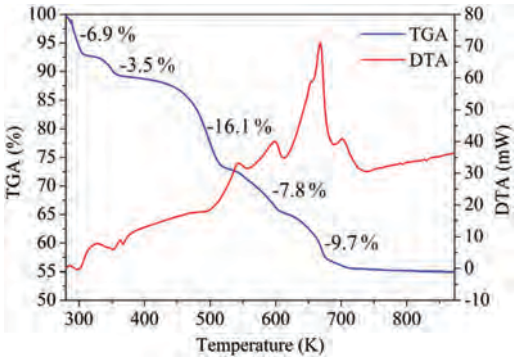

Fig. 3 TGA (blue) and DTA (red) curves of **1·MeCN** at 273–873 K in air flow. A stepwise decomposition (and combustion) of the framework is observed.

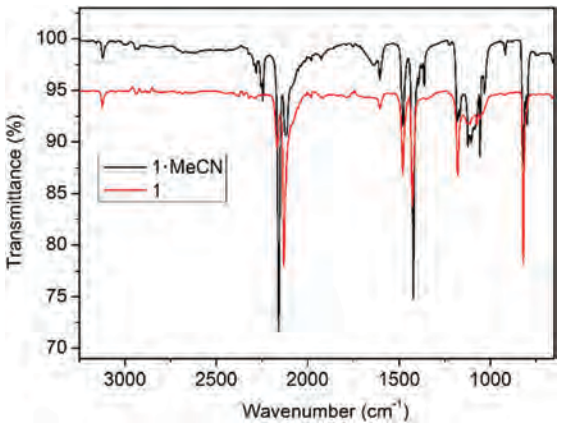

Fig. 4 IR (ATR) spectra of **1** and **1·MeCN**.

endothermic peak at 500 K. High exothermic peaks at 550–750 K correspond to the combustion of cyanide.

The IR spectra of **1** and **1·MeCN** are given in Fig. 4. Weak stretching ν_{CH} vibrations appear at 3123 cm^{-1} for the aromatic C–H of pyrazine and at 2900–3000 cm^{-1} for the CH_3 moiety of acetonitrile. The characteristic ν_{CN} bands of the nitrile group of CH_3CN are observed at 2200–2300 cm^{-1}. Bands related to the ν_{CN} stretching vibrations of the bridging cyanide appear at 2130 and 2158 cm^{-1} for both **1** and **1·MeCN**. Their relative intensities drastically change upon the **1·MeCN** to **1** transition. Intensive bands at 1478 and 1421 cm^{-1}, the latter of which shifts to 1427 cm^{-1} upon solvent loss, correspond to the ν_{CN} and ν_{CC} stretching vibrations in the pyrazine ring. Characteristic aromatic overtones, together with ν_{CN} and ν_{CC} stretching vibrations, cover the 1500–1700 cm^{-1} region. In-plane C–H bending peaks are found in the 1000–1200 cm^{-1} region, and the out-of-plane C–H bending peak is observed at 824 cm^{-1}. Acetonitrile related peaks appear at 650–1400 cm^{-1} for **1·MeCN**.

Mössbauer spectra of **1** and **1·MeCN** at 290 K are shown in Fig. 5 (left column). The spectrum of **1·MeCN** shows a typical doublet characteristic of LS iron(II) (δ = 0.341(4) mm s^{-1}, $|\Delta E_Q|$ = 0.221(9) mm s^{-1}). Upon transformation to **1**, another type of Fe centre emerges with δ = 0.231(8) mm s^{-1} and $|\Delta E_Q|$ = 0.680(15) mm s^{-1}.

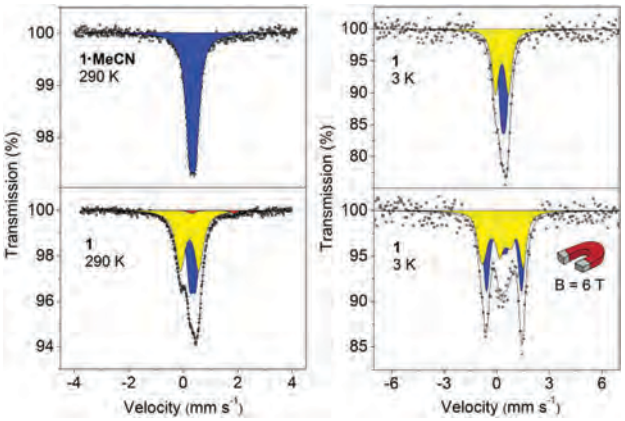

Fig. 5 Mössbauer spectra of **1·MeCN** and **1** at 290 K (left) and **1** at 3 K (right), with and without magnetic field. Two types of LS Fe(II) centres (1 : 1, shown in blue and yellow) are detected in **1**.

The ratio between the two types of Fe atoms is close to 1 : 1 (45(4) : 53(4)%). A small content (2.0(13)%) of Fe(II) HS fraction is also detected (δ = 1.09(9) mm s^{-1} and $|\Delta E_Q|$ = 1.5(2) mm s^{-1}).

Since conventional Mössbauer spectroscopy does not give conclusive answers about spin and oxidation states of newly emerging iron centres, the hyperfine field at the Fe nuclei (induced by an external magnetic field) was analysed. The 3 K spectra of **1**, acquired without and with a magnetic field of 6 T,[26] are shown in Fig. 5 (right column).

A zero-field spectrum confirms the coexistence of two types of Fe centres in a 50(10) : 50(10)% ratio, with δ = 0.39(2) mm s^{-1}, $|\Delta E_Q|$ = 0.25(5) mm s^{-1} for one and δ = 0.30(3) mm s^{-1}, $|\Delta E_Q|$ = 0.74(7) mm s^{-1} for the other. The magnetically split spectrum of **1** shows a field of 6.0(1) T at both Fe sites, *i.e.* only the applied magnetic field contributes to the hyperfine field, which is consistent with a LS configuration for Fe(II) (S = 0).‡ Despite the fact that for both Fe centres, δ is in agreement with the results of Mössbauer studies on the related Hofmann-like clathrates, the large value of ΔE_Q = −0.74 mm s^{-1} for one of the sites is compatible only with a highly distorted ligand field. Possible structural distortions in the framework (which are not seen in the PXRD, Fig. S2, ESI†) can be attributed to the solvent loss associated with two non-equivalent Fe(II) centres and the related signals in the Mössbauer spectrum. This is in harmony with the IR spectrum, revealing a strong ν_{CN} shift that is related to a distortion of the Fe coordination environment.

In conclusion, we demonstrated the SCO properties of [Fe(pz){Ag(CN)$_2$}$_2$] and [Fe(pz){Ag(CN)$_2$}$_2$]·MeCN, both of which display a transition with hysteresis at high temperatures, a rare case for complexes of the Hofmann-clathrate type. The SCO in this framework is sensitive to the inclusion of guest molecules, which makes it an interesting object of guest induced SCO studies (including chiral guest molecules[27,28]). SCO behaviour of this framework and of its recently reported gold(I) analogue open a route to very simple frameworks with spin transitions. Copper(I) analogues and complexes with substituted pyrazines[24,29] may be promising subjects for further research. The combination of different simple N-donor organic ligands with cyanometalates

may be a promising strategy to identify new SCO MOFs with molecular bistability above room temperature.

Experimental

Synthesis

A powder of **1·MeCN** was obtained by mixing $Fe(ClO_4)_2{\cdot}6H_2O$ (36.3 mg, 0.1 mmol), $KAg(CN)_2$ (39.8 mg, 0.2 mmol) and pyrazine (8 mg, 0.1 mmol) in acetonitrile/water mixture (9 : 1, 2 ml). A bright red powder of **1·MeCN** precipitates immediately. It was washed with acetonitrile and dried at room temperature for 1 h. Yield: 88%. A powder of **1** was obtained by drying **1·MeCN** at 120 °C for 15 min. Anal. calcd for **1·MeCN** $C_{10}H_7Ag_2FeN_7$: C, 24.18; N, 19.74; H, 1.42. Found: C, 23.96; N, 19.55; H, 1.30. Anal. calcd for **1** $C_8H_4Ag_2FeN_6$: C, 21.08; N, 18.44; H, 0.88. Found: C, 21.22; N, 18.97; H, 0.71.

Single crystals of **1·MeCN** were obtained by slow diffusion of $Fe(ClO_4)_2{\cdot}6H_2O$ (36.3 mg) and pyrazine (8 mg) in acetonitrile (2 ml) from one side and $KAg(CN)_2$ (39.8 mg) aqueous solution (2 ml) from the other side through a water/acetonitrile mixture (1 : 2, 4 ml). Red crystals grew on the tube walls within 2 weeks.

Single crystal XRD

XRD was performed on a Bruker SMART diffractometer (Mo-Kα) equipped with an APEX II Detektor. Structure was solved with SHELXS using the direct method and refined with SHELXL using least square methods (Olex2 environment). Non-hydrogen atoms were refined with anisotropic thermal parameters. Aromatic hydrogen atoms were placed at calculated positions and refined using a riding model. Hydrogen atoms of the idealized methyl group were placed at calculated positions.

Acknowledgements

This study was financed by the H2020 Marie Skłodowska-Curie Individual Fellowship 659614 and supported by the European Synchrotron Radiation Facility (ESRF). We also acknowledge the kind help of Dr R. Rüffer, Dr A. Chumakov and O. I. Kucheriv.

Notes and references

‡ The spectrum can be simulated using spin-Hamiltonian model for randomly oriented EFG and angle $\theta = 0^\circ$ between the direction of magnetic field and γ-rays, since the polarization vector of the Synchrotron Mössbauer beam is parallel to the external field. The isomer shift and linewidth for both Fe sites have been extracted from the zero-field spectrum and fixed during the fit, whilst in varying the quadrupole splitting $\Delta E_Q = e^2QV_{zz}/2$ the sign of V_{zz} has been found to be negative (Fig. S4, ESI†).

1 P. Gütlich and H. A. Goodwin, *Topics in Current Chemistry*, Springer, 2004, vol. 233–235.
2 P. Gütlich, *Eur. J. Inorg. Chem.*, 2013, 581–591.
3 M. A. Halcrow, *Spin-Crossover Materials: Properties and Applications*, John Wiley & Sons, 2013.
4 G. Aromí, L. A. Barrios, O. Roubeau and P. Gamez, *Coord. Chem. Rev.*, 2011, **255**, 485–546.
5 M. C. Muñoz and J. A. Real, *Coord. Chem. Rev.*, 2011, **255**, 2068–2093.
6 L. G. Lavrenova and O. G. Shakirova, *Eur. J. Inorg. Chem.*, 2013, 670–682.
7 I. A. Gural'skiy, B. O. Golub, S. I. Shylin, V. Ksenofontov, H. J. Shepherd, P. R. Raithby, W. Tremel and I. O. Fritsky, *Eur. J. Inorg. Chem.*, 2016, 3191–3195.
8 X. Bao, P.-H. Guo, W. Liu, J. Tucek, W.-X. Zhang, J.-D. Leng, X.-M. Chen, I. Gural'skiy, L. Salmon, A. Bousseksou and M.-L. Tong, *Chem. Sci.*, 2012, **3**, 1629–1633.
9 I. Šalitroš, J. Pavlik, R. Boča, O. Fuhr, C. Rajadurai and M. Ruben, *CrystEngComm*, 2010, **12**, 2361–2368.
10 R. Boča, M. Boča, L. Dlháň, K. Falk, H. Fuess, W. Haase, R. Jaroščiak, B. Papánková, F. Renz, M. Vrbová and R. Werner, *Inorg. Chem.*, 2001, **40**, 3025–3033.
11 R. Boča, F. Renz, M. Boča, H. Fuess, W. Haase, G. Kickelbick, W. Linert and M. Vrbová-Schikora, *Inorg. Chem. Commun.*, 2005, **8**, 227–230.
12 Y. Bodenthin, G. Schwarz, Z. Tomkowicz, A. Nefedov, M. Lommel, H. Möhwald, W. Haase, D. G. Kurth and U. Pietsch, *Phys. Rev. B: Condens. Matter Mater. Phys.*, 2007, **76**, 064422.
13 G. S. Matouzenko, S. A. Borshch, E. Jeanneau and M. B. Bushuev, *Chem. – Eur. J.*, 2009, **15**, 1252–1260.
14 G. Schwarz, Y. Bodenthin, Z. Tomkowicz, W. Haase, T. Geue, J. Kohlbrecher, U. Pietsch and D. G. Kurth, *J. Am. Chem. Soc.*, 2011, **133**, 547–558.
15 T. Kitazawa, Y. Gomi, M. Takahashi, M. Takeda, M. Enomoto, A. Miyazaki and T. Enoki, *J. Mater. Chem.*, 1996, **6**, 119–121.
16 V. Niel, J. M. Martinez-Agudo, M. C. Muñoz, A. B. Gaspar and J. A. Real, *Inorg. Chem.*, 2001, **40**, 3838–3839.
17 M. Ohba, K. Yoneda, G. Agustí, M. C. Muñoz, A. B. Gaspar, J. A. Real, M. Yamasaki, H. Ando, Y. Nakao, S. Sakaki and S. Kitagawa, *Angew. Chem., Int. Ed.*, 2009, **48**, 4767–4771.
18 Z. Arcís-Castillo, F. J. Muñoz-Lara, M. C. Muñoz, D. Aravena, A. B. Gaspar, J. F. Sánchez-Royo, E. Ruiz, M. Ohba, R. Matsuda, S. Kitagawa and J. A. Real, *Inorg. Chem.*, 2013, **52**, 12777–12783.
19 P. D. Southon, L. Liu, E. A. Fellows, D. J. Price, G. J. Halder, K. W. Chapman, B. Moubaraki, K. S. Murray, J.-F. Létard and C. J. Kepert, *J. Am. Chem. Soc.*, 2009, **131**, 10998–11009.
20 F. J. Muñoz Lara, A. B. Gaspar, D. Aravena, E. Ruiz, M. C. Muñoz, M. Ohba, R. Ohtani, S. Kitagawa and J. A. Real, *Chem. Commun.*, 2012, **48**, 4686–4688.
21 F. J. Muñoz-Lara, A. B. Gaspar, M. C. Muñoz, M. Arai, S. Kitagawa, M. Ohba and J. A. Real, *Chem. – Eur. J.*, 2012, **18**, 8013–8018.
22 D. Aravena, Z. A. Castillo, M. C. Muñoz, A. B. Gaspar, K. Yoneda, R. Ohtani, A. Mishima, S. Kitagawa, M. Ohba, J. A. Real and E. Ruiz, *Chem. – Eur. J.*, 2014, **20**, 12864–12873.
23 Z. Arcís-Castillo, M. C. Muñoz, G. Molnár, A. Bousseksou and J. A. Real, *Chem. – Eur. J.*, 2013, **19**, 6851–6861.
24 O. I. Kucheriv, S. I. Shylin, V. Ksenofontov, S. Dechert, M. Haukka, I. O. Fritsky and I. A. Gural'skiy, *Inorg. Chem.*, 2016, **55**, 4906–4914.
25 V. Niel, M. C. Muñoz, A. B. Gaspar, A. Galet, G. Levchenko and J. A. Real, *Chem. – Eur. J.*, 2002, **8**, 2446.

26 V. Potapkin, A. I. Chumakov, G. V. Smirnov, J.-P. Celse, R. Rüffer, C. McCammon and L. Dubrovinsky, *J. Synchrotron Radiat.*, 2012, **19**, 559–569.
27 I. A. Gural'skiy, V. A. Reshetnikov, A. Szebesczyk, E. Gumienna-Kontecka, A. I. Marynin, S. I. Shylin, V. Ksenofontov and I. O. Fritsky, *J. Mater. Chem. C*, 2015, **3**, 4737–4741.
28 I. A. Gural'skiy, O. I. Kucheriv, S. I. Shylin, V. Ksenofontov, R. A. Polunin and I. O. Fritsky, *Chem. – Eur. J.*, 2015, **21**, 18076–18079.
29 S. I. Shylin, I. A. Gural'skiy, D. Bykov, S. Demeshko, S. Dechert, F. Meyer, M. Hauka and I. O. Fritsky, *Polyhedron*, 2015, **87**, 147–155.

